Program Digest, 2019 IEEE International Ultrasonics Symposium (IUS)
Glasgow, Scotland, October 6-9, 2019

# Flow Metering of Gases Using Ultrasonic Phased-Arrays at High Velocities

Christoph Haugwitz, Axel Jäger, Gianni Allevato, Jan Hinrichs, Alexander Unger, Sebastian Saul, Johannes Brötz, Berthold Matyschok, Peter Pelz and Mario Kupnik
Technische Universität Darmstadt, Darmstadt, Germany

***Abstract*—We present an ultrasonic transit-time gas flow meter (UFM) based on our 40 kHz 8×8 phased-array. Besides single element receivers, the UFM uses a waveguide-based phased-array with an inter-element spacing of half-lambda as sender, capable of electronic beam steering for an extra-large flow velocity range. The sound drift effect limits the measurement range of conventional UFMs, i.e. we compensate the sound-drift effect using beam steering. The UFM features a maximum measurable flow velocity up to 100 m s$^{-1}$. The flowmeter body is a fully 3D-printed pipe with a length of 800 mm and an inner diameter of 315 mm. The receivers are arranged at inclination angles of 45°. The flowmeter is tested on a test rig for ventilation fans according to ISO 5801:2017(E). At zero flow velocity, the SNR for the downstream receiver is 64.1 dB. Without compensation of the sound-drift effect, at the full flow velocity of 100 m s$^{-1}$, the SNR drops down to 18.0 dB (downstream). When the compensation is enabled, the SNR raises by 18.7 dB (downstream) at full flow velocity. These numbers proof that the usage of a phased-array in a UFM can significantly increase the maximum measurable flow velocity. Further advantages are the possibility of multi-path measurements for an improved meter factor, i.e. eccentric flow meter configurations.**

## I. Introduction

Ultrasonic transit-time gas flow meters consist of one or more sound paths inclined to the gas flow direction. The time of flight required to pass a sound path depends on the flow velocity. Therefore the flow velocity can be calculated by measuring the transit times. The fact that the sound drifts away by the flow is a problem, causing a loss in received power, a lower signal-to-noise-ratio (SNR), and, thus, a decrease in measurement accuracy. The impact of the sound drift effect intensifies with increasing velocity.

Different approaches have been proposed to address the sound-drift problem. K. S. Mylvaganam [1] mechanically tilts the transmit transducer for maximum SNR. M. Kupnik et al. [2] mechanically shift the receiving transducers e.g. downstream.

We have already demonstrated a UFM, featuring active electronic beam steering for flow rates up to 41 m s$^{-1}$ using an ultrasonic phased-array (A. Jäger et al. [3]). In this paper, we extend our previous work by increasing both the diameter to 315 mm and the flow rate up to 100 m s$^{-1}$ (Fig. 1).

## II. Physical model

In order to compensate the sound-drift effect, the optimal angle for beam steering must be determined. A model for the optimal angle to steer the sound beam has been presented in [3]. It is calculated using the speed of sound c and the velocity

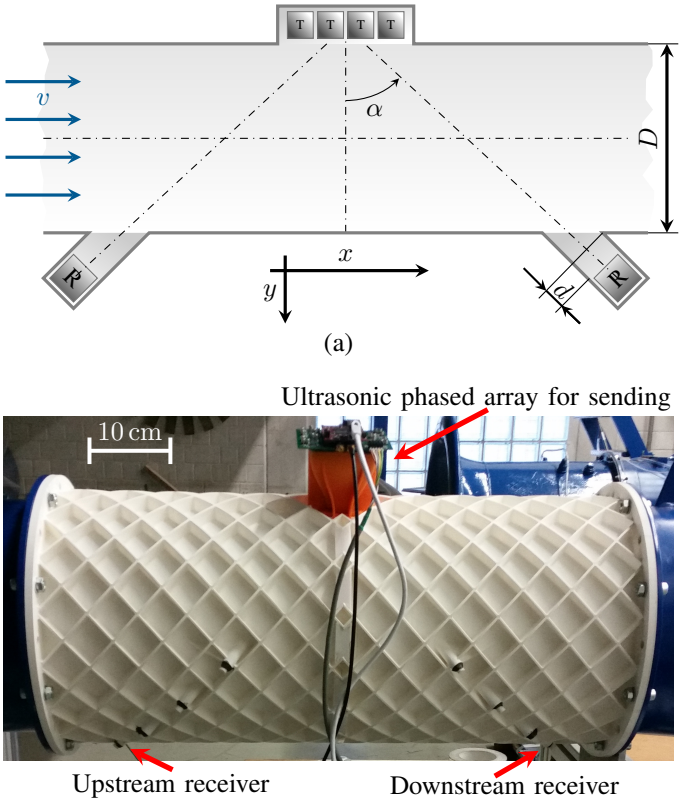


Fig. 1. The ultrasonic measuring system consists of an ultrasonic phased-array [4] and two receivers (a). Those are mounted on a 3D-printed pipe (b) with an inner diameter of $D = 315\,\mathrm{mm}$. The receivers are inclined in an angle of $\alpha = 45°$ to the array and are drawn back in their port cavities by $d = 1\,\mathrm{mm}$ (a). The pipe has additional transducer port cavities for up to 8 eccentric sound paths in each direction for future work. The 3D-printed pipe is reinforced with diagonal struts for improved stability (b).

of the flow averaged over the sound path $v_p$. In explicit form the optimal angle is

$$\phi_{\mathrm{opt}} = \arctan\left[\frac{\pm 1}{1-\left(\frac{v_p}{c}\right)^2} - \sqrt{\left(\frac{1}{1-\left(\frac{v_p}{c}\right)^2}\right)^2 - 1}\right], \quad (1)$$

with the positive sign in the numerator for the downstream receiver and the negative sign for the upstream receiver.

The models for the amplitude received are calculated with the amplitude at zero flow multiplied with the flow-dependent

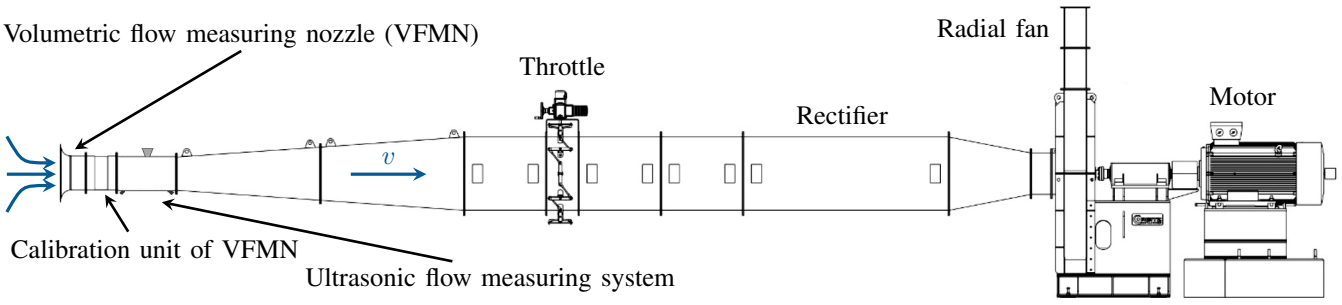


Fig. 2. The ultrasonic flow measuring system is inserted into the test rig from S. Saul [5]. The test rig is build according to norm ISO 5801:2017(E) [6]. A radial fan pumps air through the pipes. In order to avoid vortices there is a rectifier in front of the fan. The throttle is not used in this work and is left open. The volumetric flow measuring nozzle is build according to norm ISO 5167-3-2003 [7] to ensure a steady, symmetric flow. It measures the flow by measuring the pressure difference at the nozzle and it is calibrated with a prantl pitot tube by U. Kruse [8]. The measured flow is used as a reference and is compared with the flow measured by the ultrasonic flow measuring system.

attenuation factor $a(v_a)$. If the compensation of the sound-drift effect is enabled, the attenuation factor is described as a multiplication of three effects, i.e.

$$a(v_a) = a_{\mathrm{rx}} \cdot a_{\mathrm{array}} \cdot a_{\mathrm{shadow}}. \tag{2}$$

First, if the flow increases, the steering angle $\phi$ increases. The sound path that hits the receiver arrives with the same angle, and, thus, the directivity of the receiver leads to an attenuation $a_{\mathrm{rx}}$. Second, the phased-array generates less sound pressure for steeper steering angles [4] which is modelled as the attenuation $a_{\mathrm{array}}$. Third, the sound pressure is attenuated by $a_{\mathrm{shadow}}$ by the sound shadow of the transducer port cavity walls. The combination of those effects results in the flow dependent attenuation model [Fig. 3 (c1, c2), red curves].

Without compensation of the sound-drift, the phased-array steers to $\phi = \pm 45°$. Despite this, the sound path that hits the receiver starts and ends at an angle of $\phi_{\mathrm{opt}}$. Therefore $a_{\mathrm{rx}}$ and $a_{\mathrm{shadow}}$ are not influenced by the disabled compensation. The second factor $a_{\mathrm{array}}$ changes compared to the configuration with enabled compensation, because the sound drifts away and the new sound pressure at the receiver is smaller than without sound-drift effect. This is calculated using the sound-pressure distribution of the ultrasonic phased-array [4] [Fig. 3 (a1, a2), red curves].

## III. Experimental Setup

The experiment to test sound-drift compensation with an ultrasonic phased-array consists of a flow rig and the ultrasonic flow measuring system. The measurements are conducted with the same ultrasonic phased-array as in our previous work [9]. The transducer type used in the array (MA40S4S, Murata Seisakusho, Nagaokakyo, Japan) is used for the receivers as well. The amplitudes received are measured with the oscilloscope R&SScope-Rider RTH1004 (Rohde & Schwarz GmbH & Co. KG, Munich, Germany). The oscilloscope and the phased-array are connected to a PC via Ethernet.

The flow meter body is 3D-printed in two parts and glued after the printing. Both parts are 3D-printed using the FDM [10] 3D-printer Creality CR-10S5 (Creality 3D, Shenzhen, China) (Fig. 1).

The flow rig (Fig. 2) is build according to ISO 5801:2017(E) [6] and is capable of providing a volumetric airflow of around $7.8\,\mathrm{m\,s^{-3}}$. This is done by a radial fan of type KXE 250-016025-00 (Reitz Ventilatoren, Hxter, Germany). It is driven with an AC drive Sinamics G150 (Siemens AG, Berlin/Munich, Germany), providing a constant frequency for each flow velocity to have the flow rate approximately constant while measuring. The environmental conditions i.e. temperature, ambient pressure and relative humidity are measured with the combined measuring device PTU303 (Vaisala, Vantaa, Finnland).

The entrance nozzle of the flow rig is an ISA-1932 type nozzle described in DIN EN ISO 5167-3 [7] ensuring a continuous, vortex free and radial symmetric flow profile. In addition, the flow velocity is calculated from the known relationship of pressure difference across the nozzle with the formula from [7]. The differential pressure at the nozzle is measured with the Intelligent-Pressure-Scanner Model 9016 (Pressure Systems Inc., Hampton/Virginia, USA). The nozzle used has been calibrated by U. Kruse [8, p. 13] with a Prantl-pitot tube to adjust the nozzle constant $C_D$ for increased accuracy.

For each flow rate, the radial fan is set to a fixed rotation frequency. After a settle time of one minute, the ultrasonic phased-array sequentially sends a sound pulse with a length of 40 periods to the defined directions (20° to 70° in steps of 2°). During the transmission, the differential pressure at the nozzle, the environmental conditions and the received sound signals are recorded. Every data point is measured 5 times.

The flow velocity averaged over the sound path $v_p$ is calculated from the length of the sound path $L$, the upstream time $t_u$ and the downstream time $t_d$ by

$$v_p = \frac{L}{2 \cdot \sin(\alpha)} \left( \frac{t_u - t_d}{t_u \cdot t_d} \right). \tag{3}$$

The meter factor, needed to calculate the velocity averaged

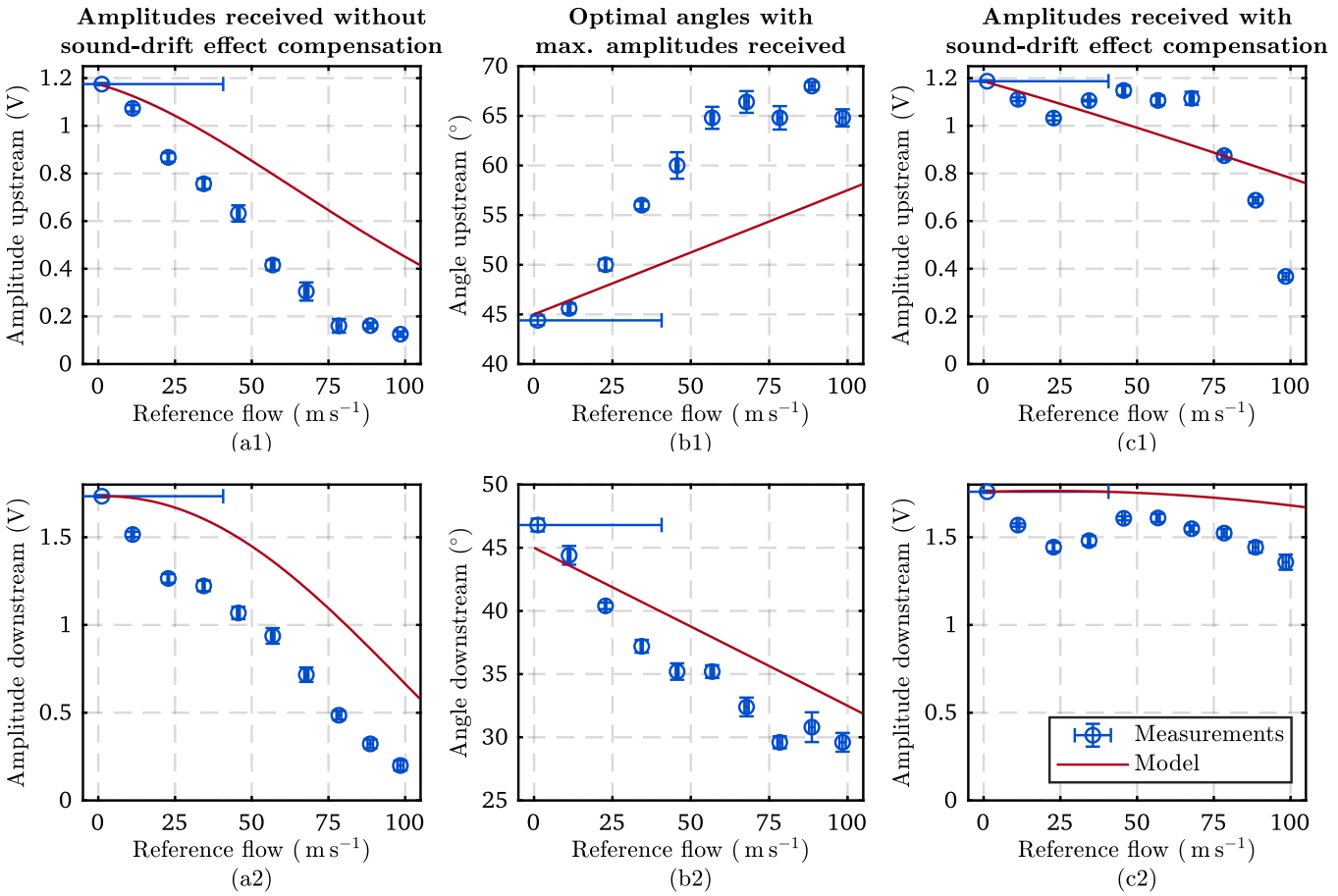


Fig. 3. First, the phased-array is sending directly to the receiver at an angle of $\alpha = \pm 45°$ without compensation of the sound-drift effect (a1, a2). Since there is no compensation, the sound beam drifts away and the amplitude drops significantly at higher flow rates. The effect has a higher impact on the upstream receiver (a1) than on the downstream receiver (a2). With steering to the angle with the highest amplitude received at the specific flow velocity $\phi_{\mathrm{opt}}$ enabled, the calculated angle deviates from $\alpha = \pm 45°$ for nonzero flow. If the array sends to the downstream receiver, an approximately linear relationship is observed (b2). When the array sends to the upstream receiver, the optimal steering angle must be larger than the model and does not increase any further at $70\,\mathrm{m\,s^{-1}}$ (b1). This happens because the phased-array can not send efficiently to more than $\alpha = \pm 70°$. The amplitude received is significantly higher at high flow rates when compensating is enabled (c). The amplitude received at the upstream receiver drops significantly faster at a flow velocity of $70\,\mathrm{m\,s^{-1}}$ and higher (c1). However, it is still higher than without compensation of the sound-drift effect (a).

over the area of the pipe $v_a$ [11], is

$$k_v = \frac{v_a}{v_p} = \frac{4}{D}\frac{\int_0^R v(r)\mathrm{d}r}{\int_0^R v(r)\mathrm{d}r}. \tag{4}$$

This is calculated with the flow profile model described in [12]

$$v(r) = v_{\max} \cdot \left[1 - \left(\frac{r}{R}\right)^{2m}\right]. \tag{5}$$

For the flow exponent $m$, the data of the flow profile from the calibration of the nozzle [8] is fitted, so that

$$m = 8.789 \cdot \log_{10}(v_a) + 20.94 \tag{6}$$

is satisfied. For the flow velocity required for calculating $m$, the reference flow measured at the nozzle is used. The arrival times $t_d$ and $t_u$ are measured using a threshold approach.

## IV. Results

The experiment is divided into two parts. First, the ultrasonic phased-array steers to $\alpha = \pm 45°$ only, imitating a conventional UFM. Second, the array uses the angle of the highest amplitudes received in order to compensate the sound-drift effect. With compensation enabled, the amplitude and therefore the SNR of the receiving signal is exceeding the amplitude without compensation (Fig. 3). At a flow rate of $v = 0\,\mathrm{m\,s^{-1}}$, the SNR is 61.6 dB for the upstream and 61.6 dB for the downstream case, respectively. With no compensation enabled at $v = 100\,\mathrm{m\,s^{-1}}$ the SNR is 18.0 dB for the downstream case and 24.4 dB for the upstream case, respectively. If steering is enabled, the SNR increases to 30.8 dB for the upstream case and to 36.7 dB for the downstream case. Afterwards the flow measured is calculated for the experiment demonstrating the sound-drift compensation (Fig. 4).

## V. Discussion

In this work, gas flow velocities up to $100\,\mathrm{m\,s^{-1}}$ are measured with the ultrasonic transit-time method which corresponds to 29 % of the speed of sound.

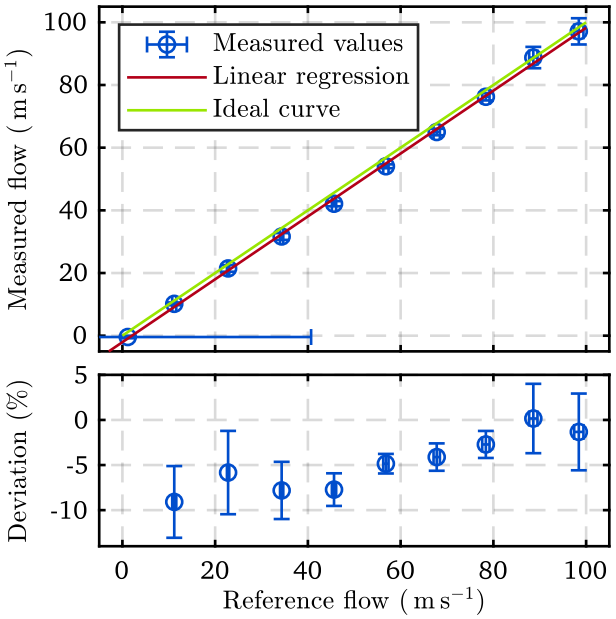


Fig. 4. The flow velocity is measured with compensation of the sound-drift effect enabled. The deviation (bottom) of the ideal curve is higher for lower flow rates. The linear regression (red) is calculated to $v_m(v_f) = 1.004 \cdot v_f - 2.074\,\mathrm{m\,s^{-1}}$. The $r$-square value of the linear regression is $r^2 = 0.9990$ and the root mean squared error is $s_{\mathrm{rmse}} = 1.1431\,\mathrm{m\,s^{-1}}$. Therefore, the connection between the measured and the reference flow can be considered linear. The ideal curve (green) has a gradient of 1 and crosses the origin. The uncertainties are best in the range of $v = 50\,\mathrm{m\,s^{-1}}$ to $v = 80\,\mathrm{m\,s^{-1}}$. For lower flow rates, the uncertainty increases to $\pm 4.9\,\%$ as well as for for flow rates above $v = 90\,\mathrm{m\,s^{-1}}$ up to $\pm 4.3\,\%$.

The results of this paper extend our previous work [3] in terms of measured data points, uncertainty estimations and a higher range of up to $100\,\mathrm{m\,s^{-1}}$ compared to $41\,\mathrm{m\,s^{-1}}$. As mentioned before, mechanical adjustments for actively compensating the sound drift effect as in [1], [2] are not necessary using the method described. Therefore, it is less error-prone and more durable since there is no mechanical wear. The high uncertainty of the reference flow at zero flow of $\pm 39.53\,\mathrm{m\,s^{-1}}$ (Fig. 3) is caused by the flow which is proportional to the square root of the difference pressure [7]. This is linearly interpolated in the uncertainty calculation and leads to a higher error at $0\,\mathrm{m\,s^{-1}}$. However, the flow rig was turned off during that measurement, so the flow velocity can be assumed to be zero.

There is a difference between the theoretical and measured optimal angle $\phi_{\mathrm{opt}}$ at the upstream receiver of up to 12° at a flow of $60\,\mathrm{m\,s^{-1}}$ [Fig. 3(b1)]. One reason are imperfections of the ultrasonic phased-array caused by differences in the sensitivities and phase responses of the individual transducers that lead to a distorted directivity at higher angles. At higher flow rates, the optimal angle $\phi_{\mathrm{opt}}$ measured does not increase any further at $v = 70\,\mathrm{m\,s^{-1}}$, because the phased-array can not send efficiently at higher angles than 65°. Hence, the compensation of the sound-drift effect is limited and the amplitude at the receiver drops significantly [Fig. 3(c1)].

One possible reason for the uncertainty of the measured flow velocity (Fig. 4) is a small oscillating change in flow due to the rotating fan. It leads to a change of the attenuation on the sound path at each repetition of the measurement. Since the transit-time is calculated with a threshold approach, it changes slightly at different attenuations.

## VI. Conclusion and Outlook

Our approach is promising because the SNR is higher if the sound-drift effect is compensated using an ultrasonic phased-array at high flow rates, compared to the SNR without compensation. Thus, it is possible to increase the maximum measurable velocity with an ultrasonic phased-array. Further, our experiment shows the feasibility of using 3D-printing for flow metering, which enables high design flexibility at low cost.

Future work includes measurement of flow using the 8 off-centric sound paths that are included in the pipe as well. Furthermore, simulating sound wave propagation in the pipe allows to optimize the measurement uncertainty. Sending a sound pulse with a changing frequency allows to determine the transit time with a matched filter at a higher accuracy. For measuring even higher flow rates, the receiving transducers can be additionally shifted downstream linearly as shown in [2]. In addition, lowering the angle $\alpha$ from $\alpha = 45°$ to $\alpha = 30°$ enables a wider range of steering angles to be selected for drift compensation.

## References

[1] K. S. Mylvaganam. High-rangeability ultrasonic gas flowmeter for monitoring flare gas. *IEEE Transactions on Ultrasonics, Ferroelectrics, and Frequency Control*, 36(2):144–149, 1989.

[2] M. Kupnik, A. Schroder, and M. Groschl. PS-16 Adaptive Asymmetric Double-Path Ultrasonic Transit-Time Gas Flowmeter. In *2006 IEEE Ultrasonics Symposium*, pages 2429–2432, 2006.

[3] A. Jäger, A. Unger, H. Wang, Y. Arnaudov, L. Kang, R. Su, D. Lines, S. N. Ramadas, S. Dixon, and M. Kupnik. Ultrasonic phased array for sound drift compensation in gas flow metering. In *2017 IEEE International Ultrasonics Symposium (IUS)*, pages 1–4, 2017.

[4] A. Jäger. *Airborne ultrasound phased arrays*. PhD thesis, TU Darmstadt, 2018.

[5] S. Saul, B. Matyschok, and P. Pelz. fan model test at varying ambient pressure: efficient product validation at full scale reynolds and mach number. *In FAN2018 - Proceedings of the International Conference on Fan Noise, Aerodynamics, Applications and Systems*, 2018.

[6] Fans Performance testing using standardized airways [ISO 5801:2017(E)], 2017.

[7] Measurement of fluid flow by means of pressure differential devices inserted in circular cross-section conduits running full Part 3: Nozzles and Venturi nozzles (ISO 5167-3:2003), 2004.

[8] U. Kruse. *Experimental Investigation of a Centrifugal Fan to the Influence of the Mach Number Effect*. Master's thesis, Chair of Fluid Systems, TU Darmstadt, 2015.

[9] A. Jäger, D. Großkurth, M. Rutsch, A. Unger, R. Golinske, H. Wang, S. Dixon, K. Hofmann, and M. Kupnik. Air-coupled 40-khz ultrasonic 2D-phased array based on a 3D-printed waveguide structure. In *2017 IEEE International Ultrasonics Symposium (IUS)*, pages 1–4. IEEE, 2017.

[10] S. S. Crump. Modeling apparatus for three-dimensional objects, August 23. US Patent 5,340,433, 1994.

[11] L. C. Lynnworth. *Ultrasonic measurements for process control: theory, techniques, applications*. Academic press, 1989.

[12] J. Gätke. *Akustische Strömungs- und Durchflussmessung*. Akad.-Verlag, Berlin, 1991.